

Design and Structure Analysis of Artificial Metalloproteins: Selective Coordination of His64 to Copper Complexes with Square-Planar Structure in the *apo*-Myoglobin Scaffold

Satoshi Abe,[†] Takafumi Ueno,^{†,‡} Pattubala A. N. Reddy,[†] Seiji Okazaki,[§] Tatsuo Hikage,^{||} Atsuo Suzuki,[§] Takashi Yamane,[§] Hiroshi Nakajima,[†] and Yoshihito Watanabe^{*,||}

Department of Chemistry, Graduate School of Science, Department of Biotechnology, Graduate School of Engineering, High Intensity X-ray Diffraction Laboratory, and Research Center for Materials Science, Nagoya University, Nagoya 464-8602, Japan, and PRESTO, Japan Science and Technology Agency (JST), Saitama 332-0012, Japan

Received February 13, 2007

apo-Myoglobin (*apo*-Mb) was reconstituted with three copper complexes: Cu^{II}(Sal-Phe) (**1**; Sal-Phe = *N*-salicylidene-*L*-phenylalanato), Cu^{II}(Sal-Leu) (**2**; Sal-Leu = *N*-salicylidene-*L*-leucinato), and Cu^{II}(Sal-Ala) (**3**; Sal-Ala = *N*-salicylidene-*L*-alanato). The crystal structures of **1**·*apo*-Mb (1.65 Å resolution) and **2**·*apo*-Mb (1.8 Å resolution) show that the coordination geometry around the Cu^{II} atom in *apo*-Mb is distorted square-planar with tridentate Sal-X and a N^ε atom of His64 in the *apo*-Mb cavity and the plane of these copper complexes is perpendicular to that of heme. These results suggest that the *apo*-Mb cavity can hold metal complexes with various coordination geometries.

Molecular design of artificial metalloproteins and metalloenzymes is one of the goals of bioinorganic chemistry. There have been many reports that described protein composites containing metal catalysts, inhibitors linked to metal complexes, and modified metal cofactors.^{1–6} However, detailed structural analyses as well as mechanistic aspects are still not clear for most of the composites. X-ray crystal structure studies of artificial metalloproteins are essential to

improving catalytic activities and to understanding physical properties and for further application to biotechnology.^{6–13}

Myoglobin (Mb) is a small heme protein that functions as an O₂ storage unit, and it has been used as a model for many heme enzymes. Functions and structures of wild-type and its various mutants have been investigated very well;^{14–16} thus, Mb is a good candidate for a protein scaffold hosting synthetic metal active centers. For example, introduction of a copper binding site near the heme and chemical modification of the heme prosthetic group were reported while their crystal structures are not available.^{17–20}

On the other hand, we have reported a novel method for the reconstitution of *apo*-Mb with synthetic metal centers and a series of crystal structures of M^{III}(3,3′-Me₂-salophen)

- (7) Calderone, V.; Casini, A.; Mangani, S.; Messori, L.; Orioli, P. L. *Angew. Chem., Int. Ed.* **2006**, *45*, 1267–1269.
- (8) Ueno, T.; Ohashi, M.; Kono, M.; Kondo, K.; Suzuki, A.; Yamane, T.; Watanabe, Y. *Inorg. Chem.* **2004**, *43*, 2852–2858.
- (9) Ueno, T.; Koshiyama, T.; Ohashi, M.; Kondo, K.; Kono, M.; Suzuki, A.; Yamane, T.; Watanabe, Y. *J. Am. Chem. Soc.* **2005**, *127*, 6556–6562.
- (10) Ueno, T.; Yokoi, N.; Unno, M.; Matsui, T.; Tokita, Y.; Yamada, M.; Ikeda-Saito, M.; Nakajima, H.; Watanabe, Y. *Proc. Natl. Acad. Sci. U.S.A.* **2006**, *103*, 9416–9421.
- (11) Hunter, T. M.; McNae, I. W.; Liang, X. Y.; Bella, J.; Parsons, S.; Walkinshaw, M. D.; Sadler, P. J. *Proc. Natl. Acad. Sci. U.S.A.* **2005**, *102*, 2288–2292.
- (12) McNae, I. W.; Fishburne, K.; Habtemariam, A.; Hunter, T. M.; Melchart, M.; Wang, F. Y.; Walkinshaw, M. D.; Sadler, P. J. *Chem. Commun.* **2004**, 1786–1787.
- (13) Contakes, S. M.; Juda, G. A.; Langlely, D. B.; Halpern-Manners, N. W.; Duff, A. P.; Dunn, A. R.; Gray, H. B.; Dooley, D. M.; Guss, J. M.; Freeman, H. C. *Proc. Natl. Acad. Sci. U.S.A.* **2005**, *102*, 13451–13456.
- (14) Takano, T. *J. Mol. Biol.* **1977**, *110*, 537–568.
- (15) Watanabe, Y.; Ueno, T. *Bull. Chem. Soc. Jpn.* **2003**, *76*, 1309–1322.
- (16) Pfister, T. D.; Ohki, T.; Ueno, T.; Hara, I.; Adachi, S.; Makino, Y.; Ueyama, N.; Lu, Y.; Watanabe, Y. *J. Biol. Chem.* **2005**, *280*, 12858–12866.
- (17) Sigman, J. A.; Kwok, B. C.; Lu, Y. *J. Am. Chem. Soc.* **2000**, *122*, 8192–8196.
- (18) Neya, S.; Funasaki, N.; Imai, K. *J. Biol. Chem.* **1988**, *263*, 8810–8815.
- (19) Hayashi, T.; Hitomi, Y.; Ando, T.; Mizutani, T.; Hisaeda, Y.; Kitagawa, S.; Ogoshi, H. *J. Am. Chem. Soc.* **1999**, *121*, 7747–7750.

* To whom correspondence should be addressed. E-mail: yoshi@nucc.cc.nagoya-u.ac.jp. Phone: +81-52-789-3049. Fax: +81-52-789-2953.

[†] Department of Chemistry, Graduate School of Science, Nagoya University.

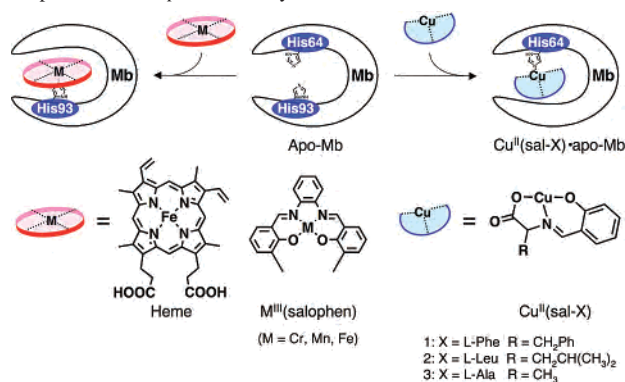
[‡] PRESTO, Japan Science and Technology Agency (JST), Japan.

[§] Department of Biotechnology, Graduate School of Engineering, Nagoya University.

^{||} High Intensity X-ray Diffraction Laboratory, Nagoya University.

[‡] Research Center for Materials Science, Nagoya University.

- (1) Lu, Y. *Angew. Chem., Int. Ed.* **2006**, *45*, 5588–5601.
- (2) Thomas, C. M.; Ward, T. R. *Chem. Soc. Rev.* **2005**, *34*, 337–346.
- (3) Ohashi, M.; Koshiyama, T.; Ueno, T.; Yanase, M.; Fujii, H.; Watanabe, Y. *Angew. Chem., Int. Ed.* **2003**, *42*, 1005–1008.
- (4) Ueno, T.; Koshiyama, T.; Abe, S.; Yokoi, N.; Ohashi, M.; Nakajima, H.; Watanabe, Y. *J. Organomet. Chem.* **2007**, *692*, 142–147.
- (5) Hayashi, T.; Hisaeda, Y. *Acc. Chem. Res.* **2002**, *35*, 35–43.
- (6) Debreczeni, J. E.; Bullock, A. N.; Atilla, G. E.; Williams, D. S.; Bregman, H.; Knapp, S.; Meggers, E. *Angew. Chem., Int. Ed.* **2006**, *45*, 1580–1585.

Scheme 1. Various Binding Geometries of Incorporated Metal Complexes in the *apo*-Mb Cavity

(salophen = *N,N'*-bis(salicylidene)-1,2-phenylenediamine, $M = \text{Cr, Mn, Fe}$) complexes bound to the *apo*-Mb cavity by noncovalent interactions.^{3,8,9} The crystal structures of these composites show that the salophen complexes tightly ligate to the heme cavity by its ligation to the proximal His93. Hydrophobic interactions such as π - π and $\text{CH}-\pi$ with adjacent amino acid residues are also observed.^{8,9}

While the molecular structures of $M(\text{salophen})$ complexes are very different from that of heme, their coordination geometries are quite similar to that of heme, i.e., planar four-coordinate ligands and the use of the proximal histidine (His93) as an axial ligand. Thus, we have extended our studies to other metal complexes preferring four-coordinate structures. We have prepared three copper(II) complexes having tridentate ligands and examined their reconstitution with *apo*-Mb. The Cu^{II} atom in $\text{Cu}^{II}(\text{Sal-X})$ ($\text{Sal-X} = N$ -salicylideneaminoacidato) prefers a square-planar or square-pyramidal structure with a nitrogen-containing donor ligand.^{21–24} In this Communication, we report the preparation of $\text{Cu}^{II}(\text{Sal-Phe})$ (**1**)·*apo*-Mb, $\text{Cu}^{II}(\text{Sal-Leu})$ (**2**)·*apo*-Mb, and $\text{Cu}^{II}(\text{Sal-Ala})$ (**3**)·*apo*-Mb and the crystal structures of **1**·*apo*-Mb and **2**·*apo*-Mb to elucidate the coordination structures induced by noncovalent interactions in the *apo*-Mb cavity. We have found that these copper(II) complexes are bound to the distal His64 with square-planar geometry and different orientation from that of heme (Scheme 1).

$\text{Cu}^{II}(\text{Sal-X})$ ·*apo*-Mb composites were prepared by a method reported by us with some modifications.³ The 1:1 composites of copper complexes with *apo*-Mb were confirmed by electrospray ionization time-of-flight mass spectrometry (see the Supporting Information). The UV–visible spectra of these composites show a broad d–d band centered at 600 nm and a charge-transfer band near 370 nm, which are commonly observed for copper(II) complexes.^{21,24} The electron paramagnetic resonance (EPR) spectra of **1**·*apo*-

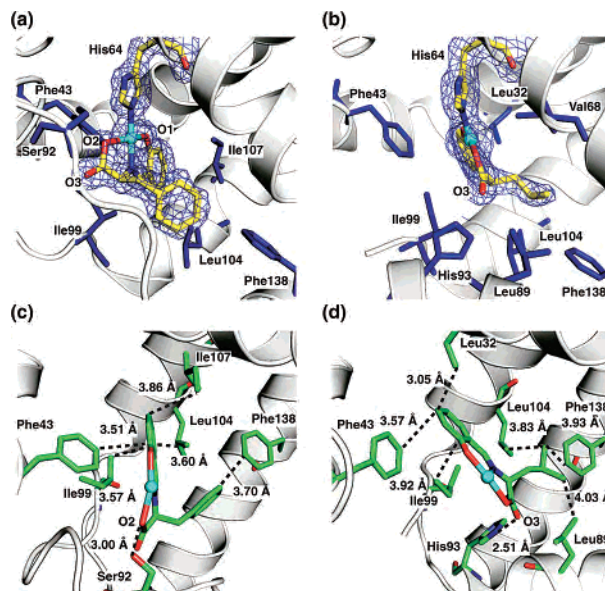


Figure 1. Active site structures of **1**·*apo*-Mb (a) and **2**·*apo*-Mb (b). The selected electron density maps (blue) of copper complexes and His64. The Cu^{II} atom is colored cyan. The $2|F_o| - |F_c|$ electron densities are contoured at 1σ . Specific interactions of **1**·*apo*-Mb (c) and **2**·*apo*-Mb (d). The interactions are shown as broken lines.

Mb, **2**·*apo*-Mb, and **3**·*apo*-Mb ($g_{\parallel} = 2.25, 2.25,$ and $2.25,$ $A_{\parallel} = 168, 171,$ and 169 G, and $g_{\perp} = 2.06, 2.06,$ and $2.06,$ respectively) indicate that the coordination geometries of **1–3** are conserved with a square-planar or square-pyramidal structure^{21,24} in *apo*-Mb, while several uncertain species were observed in the EPR spectrum of **1** in the absence of *apo*-Mb (Figure S2 in the Supporting Information). In order to compare the thermal stabilities of $\text{Cu}^{II}(\text{Sal-X})$ ·*apo*-Mb's, melting temperatures (T_m) were determined by circular dichroism spectra measurements at various temperatures. T_m 's are 68.3, 69.1, and 69.6 °C for **1**·*apo*-Mb, **2**·*apo*-Mb, and **3**·*apo*-Mb, respectively. These results suggest that the X residue in $\text{Cu}^{II}(\text{Sal-X})$ complexes does not have a large influence on the thermal stabilities of the composites.

Finally, crystal structures of **1**·*apo*-Mb and **2**·*apo*-Mb were determined with the diffraction data of 1.65 and 1.8 Å resolution, respectively. The X-ray data and refinement statistics of these crystals are summarized in Table S1 in the Supporting Information. As shown in parts a and b of Figure 1, these copper complexes are bound to the N^{ϵ} atom of distal His64 while heme and $M^{III}(\text{salophen})$ bind to that of His93.^{8,9}

The Cu–N distances in **1**·*apo*-Mb and **2**·*apo*-Mb are 1.93 and 2.06 Å, respectively, which are comparable to those of $\text{Cu}^{II}(\text{Sal-Phe})(\text{piperidine})$ (2.02 Å), $\text{Cu}^{II}(\text{Sal-Val})(3\text{-Me-Im})$ (1.96 Å), and $\text{Cu}^{II}(\text{Sal-Ala})(\text{pyrazole})$ (1.96 Å) (Table S2 in the Supporting Information).^{22–24} On the other hand, the angle of O1–Cu–O2 in **1**·*apo*-Mb (163.91°) is narrower than those of **2**·*apo*-Mb (172.81°) and the copper complexes (174 – 177°) because of the hydrogen bond interaction between O2 of **1** with O^{ν} of Ser92 (Figure 1c and Table S2 in the Supporting Information).

The plane (CuN_2O_2) of $\text{Cu}^{II}(\text{Sal-X})$ in *apo*-Mb is perpendicular to the heme plane (FeN_4), as shown in Figure 2. The

(20) Hu, Y. Z.; Tsukiji, S.; Shinkai, S.; Oishi, S.; Hamachi, I. *J. Am. Chem. Soc.* **2000**, *122*, 241–253.

(21) Garcia-Raso, A.; Fiol, J. J.; Badenas, F.; Lago, E.; Molins, E. *Polyhedron* **2001**, *20*, 2877–2884.

(22) Butcher, R. J.; Mockler, G. M.; McKern, O. *Acta Crystallogr., Sect. E* **2003**, *59*, M61–M63.

(23) Warda, S. A.; Friebe, C.; Sivy, J.; Plesch, G.; Blahova, M. *Acta Crystallogr., Sect. C* **1997**, *53*, 50–54.

(24) Plesch, G.; Friebe, C.; Warda, S. A.; Sivy, J.; Svajlenova, O. *Transition Met. Chem.* **1997**, *22*, 433–440.

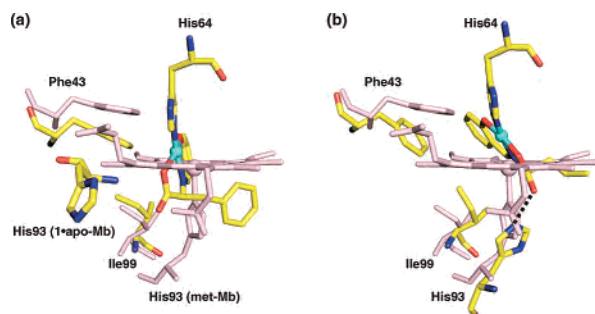


Figure 2. Superposition of the active site of *met*-Mb (pink), **1·apo-Mb** (a) and **2·apo-Mb** (b). The coordination of *met*-Mb is taken from PDB 4MBN.

heme exhibits an octahedral structure around the Fe atom in the *apo*-Mb cavity with the ligation to proximal His93 and a water molecule. On the other hand, the coordination geometry around the Cu atom in $\text{Cu}^{\text{II}}(\text{Sal-X})\cdot\text{apo-Mb}$ is distorted square-planar with a tridentate Sal-X ligand and a N^{ϵ} atom of His64. His93 in **1·apo-Mb** is exposed to the surface due to steric hindrance with Phe of **1**, while a hydrogen bond between the N^{ϵ} atom of His93 and O3 of **2** is observed in **2·apo-Mb**. The distances of the Cu atoms in **1·apo-Mb** and **2·apo-Mb** from the heme Fe are 1.59 and 2.12 Å, respectively. Thus, the copper complexes ligate to *apo*-Mb with quite different coordination structures from heme.

CH- π and π - π interactions of a benzene ring in the salicylidene moiety of Sal-X with Phe43, Ile99, Leu104, and Ile107 for **1** and Leu32, Phe43, and Ile99 for **2** seem to be very important factors to fix $\text{Cu}^{\text{II}}(\text{Sal-X})$ in *apo*-Mb, as shown in parts c and d of Figure 1. Several amino acids also interact with the X residue of $\text{Cu}^{\text{II}}(\text{Sal-X})$ such as Phe138 for **1** and Leu89, Leu104, and Phe138 for **2** (Figure 1c,d). The side chains of Phe43 and Ile99 of **1·apo-Mb** and **2·apo-Mb** shift toward the benzene ring to fix the copper complexes (Figure 2). These two residues seem to adjust the binding of **1** and **2** in the heme cavity. Apparently, the geometries and positions of **1** and **2** in the *apo*-Mb cavity are restricted by the specific interactions with surrounding amino acid residues.

The superimposed structures of **1·apo-Mb** and **2·apo-Mb** with *met*-Mb are shown in Figure 3. The root-mean-square deviations (rmsd's) of the C^{α} atoms of **1·apo-Mb** and **2·apo-Mb** from *met*-Mb are 2.34 and 0.86 Å, respectively. The value of **1·apo-Mb** is quite larger than those reported for $\text{Fe}^{\text{III}}(3,3'\text{-Me}_2\text{-salophen})\cdot\text{apo-A71GMb}$ (0.62 Å), $\text{Mn}^{\text{III}}(3,3'\text{-Me}_2\text{-salophen})\cdot\text{apo-A71GMb}$ (0.77 Å), $\text{Fe}^{\text{III}}(\text{porphyrin})\cdot\text{apo-Mb}$ (0.77 Å), and biliverdin·*apo*-Mb (0.60 Å).^{8,9,25,26} Evidently, the significant differences are observed in the C^{α} positions between His81 and Lys98, which compose an F

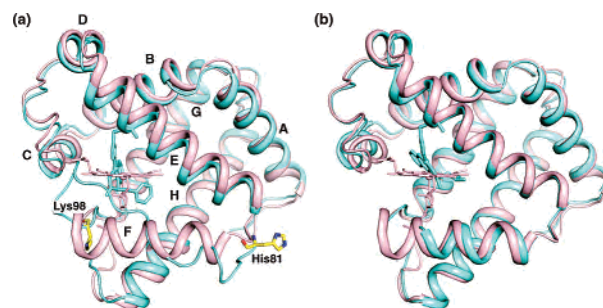


Figure 3. Superposition of the crystal structures of **1·apo-Mb** (blue) and *met*-Mb (pink) (a) and **2·apo-Mb** (blue) and *met*-Mb (pink) (b). The residues 94–97 of **2·apo-Mb** were not decided because of their disordered electron density.

helix (Figure 3a). In addition, the helical structure was completely disrupted because of the steric hindrance of **1** with His93 (Figures 2a and 3a). The unusual behavior of **1·apo-Mb** suggests that not only the active site but also the whole Mb structure are tolerant of conformational changes when a metal complex is incorporated into the cavity. In contrast, the same region in **2·apo-Mb** maintains a α -helical structure such as *met*-Mb with a small rmsd value (Figure 3b). These different structures between **1·apo-Mb** and **2·apo-Mb** suggest that the protein folding can be influenced by the ligand structure.

In summary, we have succeeded in the incorporation of copper complexes into *apo*-Mb with different coordination geometries from heme. The X-ray crystal structures of **1·apo-Mb** and **2·apo-Mb** demonstrate that **1** and **2** are fixed by ligation to the distal His64 with square-planar geometry, and side chains in the cavity are considerably flexible to stabilize the copper complexes. The results imply that *apo*-Mb is capable of accommodating various metal complexes, such as organometallic complexes.²⁷ Although we attempted to reduce the copper(II) complexes with ascorbic acid, the formation of copper(I) species was not observed. We are exploiting catalytic activities of the composites.

Acknowledgment. This work was supported by the 21st Century COE program of Nagoya University for S.A., a Grant-in-Aid for Scientific Research (Grant 18685019 for T.U.) and on Priority Areas (Grant 16033226, “Chemistry of Coordination Space” for Y.W.) from Ministry of Education, Culture, Sports, Science and Technology, Japan, and PRESTO, Japan Science and Technology Agency (JST).

Supporting Information Available: Experimental details and X-ray crystallographic data. This material is available free of charge via the Internet at <http://pubs.acs.org>.

IC070289M

(26) Neya, S.; Funasaki, N.; Sato, T.; Igarashi, N.; Tanaka, N. *J. Biol. Chem.* **1993**, *268*, 8935–8942.

(27) Satake, Y.; Abe, S.; Okazaki, S.; Ban, N.; Hikage, T.; Ueno, T.; Nakajima, H.; Suzuki, A.; Yamane, T.; Nishiyama, H.; Watanabe, Y., unpublished data.

(25) Wagner, U. G.; Muller, N.; Schmitzberger, W.; Falk, H.; Kratky, C. *J. Mol. Biol.* **1995**, *247*, 326–337.